PERGAMON

Vision Research 43 (2003) 549–561

Vision Research

www.elsevier.com/locate/visres

Attentional selection of overlapped shapes: a study using brief shape aftereffects

Satoru Suzuki *

Department of Psychology, Northwestern University, 2029 Sheridan Rd., Evanston, IL 60208, USA

Received 17 December 2001; received in revised form 10 September 2002

Abstract

Prior studies using brief stimulus sequences revealed "opponent shape aftereffects", indicative of direct opponent coding of global shape attributes such as aspect ratio, skew, taper, curvature, and convexity (perhaps in IT). Further, aftereffects from overlapped opponent pairs of adaptor shapes (e.g., concave and convex shapes) were substantially modulated by attention [Vision Res. 41 (2001) 3883]. Hypothetically, (1) attention might weight the attended and ignored contours at early stages of processing, or (2) it might sway opposing neural activity (e.g., of convex- vs. concave-tuned units) at the stage of opponent shape coding. Attentional modulation was equivalent for opponent pairs (producing opposite aftereffects) and non-opponent pairs (producing orthogonal aftereffects) of overlapped adaptor shapes, whether convexity or aspect-ratio aftereffects were measured. Further, the degree of attentional modulation obtained for these aftereffects (~60%) was comparable to that obtained for V4 cells [J. Neurosci. 19 (1999) 1736]. Taken together, differential contour weighting appears to be the primary mechanism of attentional modulation of brief shape aftereffects.

Keywords: Adaptation; Aftereffect; Aspect ratio; Attention; Convexity; Overlapped shape

1. Introduction

Recently, Suzuki (1999, 2001) reported that opponent "convexity aftereffects" induced by brief adaptation to overlapped concave and convex adaptors (measured with brief stimulus sequences) were strongly modulated by selective attention. Attentional modulation was apparent on a trial to trial basis and was as large as 40–60% of what would be observed with perfect selection (estimated with singly presented adaptors). The purpose of the current study was twofold: (1) to generalize the strong attentional modulation of convexity aftereffects to a different shape attribute (aspect-ratio aftereffects), and (2) to investigate the potential mechanism of this substantial attentional modulation of brief adaptation to shape attributes.

"Opponent shape aftereffects" refer to phenomena in which adaptation to a certain value of shape attribute (e.g., convex shape) distorts a subsequently presented neutral test shape in a repulsive manner (e.g., makes it appear concave). The first systematic evidence of adaptation to a two-dimensional image attribute (not explained by local contour adaptation) was reported by Regan and Hamstra (1992) (also see Hartmann, 1955; Kohler & Wallach, 1944; Frome, Levinson, Danielson, & Clavadetscher, 1979 for similar phenomena). By examining both the discriminability and aftereffects of vertical and horizontal elongation while the scale and the exact shape (e.g., ellipses vs. rectangles) of the stimuli were varied, Regan and Hamstra provided evidence that the visual system has a mechanism to directly code global aspect ratio. Their results were also consistent with the idea that aspect ratio is coded in an opponent manner such that the perceived aspect ratio is determined by the relative activity of two opponent populations of neural units, those tuned to horizontal elongation and those tuned to vertical elongation. [1]

* Tel.: +1-847-467-1271; fax: +1-847-491-7859.
E-mail address: satoru@northwestern.edu (S. Suzuki).

[1] Regan and Hamstra (1992) found that aspect ratio discrimination was maximal around the neutral aspect ratio (unity) and gradually deteriorated for higher and lower aspect ratios. Because it is reasonable to assume that discrimination should be most efficient where the underlying tuning curves are steepest, the result (suggesting aspect ratio tuning curves are steepest at the neutral aspect ratio) is consistent with aspect ratio coding based on two groups of cells broadly tuned to opposite (tall and flat) aspect ratios.

0042-6989/03/$ - see front matter
doi:10.1016/S0042-6989(02)00683-1

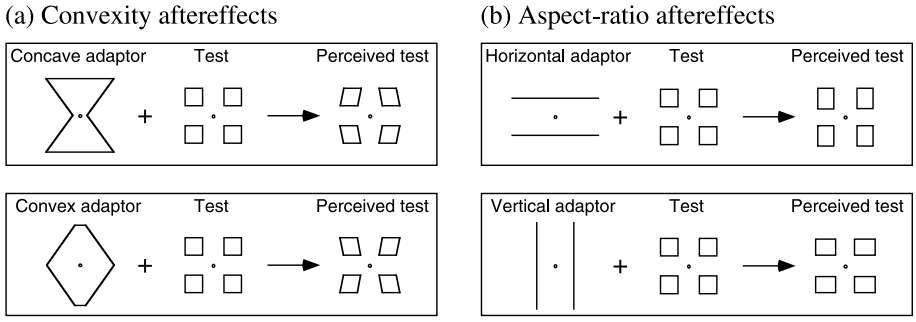

Fig. 1. Schematic drawings showing convexity aftereffects (a) and aspect-ratio aftereffects (b). (a) Top, the (concave) hourglass adaptor distorts the test pattern to appear convex. Bottom, the (convex) diamond adaptor distorts the test pattern to appear concave. (b) Top, the horizontally elongated adaptor distorts the test pattern to appear vertically elongated. Bottom, the vertically elongated adaptor distorts the test pattern to appear horizontally elongated.

Aspect-ratio aftereffects could then be explained on the basis of an activation-based reduction in sensitivity. For example, following adaptation to a vertically elongated adaptor, the "vertical-elongation-tuned" units would become less sensitive and a subsequently presented symmetric test pattern would appear horizontally elongated because "horizontal-elongation-tuned" units would respond relatively more strongly than the adapted "vertical-elongation-tuned" units (see Regan & Hamstra, 1992, for details).

Similar opponent shape aftereffects have been subsequently demonstrated for other shape attributes such as taper, curvature, skew, and convexity as well as for aspect ratio (e.g., Suzuki, 1999, 2001; Suzuki & Cavanagh, 1998). So long as the adaptor and the test stimuli were presented briefly in a rapid sequence (30–134 ms adaptation, 200 ms blank ISI, and 30–60 ms test followed by a whole-field random-dot mask), these shape aftereffects were relatively position invariant (occurring across spatial gaps of up to 12° under appropriate conditions; Suzuki & Cavanagh, 1998), tolerant for scale changes (occurring for adapt/test size ratios of 0.3–1.8; Rivest, Intriligator, Suzuki, & Warner, 1998; Suzuki, 2001), and transferred across different defining surface attributes (color-defined, luminance-defined, or high-pass filtered; Rivest, Intriligator, Warner, & Suzuki, 1997; Suzuki, 2001). These characteristics suggested that the opponent coding originally proposed for aspect ratio by Regan and Hamstra (1992) also exists for coding of other global geometric attributes which similarly represent systematic deviations from symmetry in opponent directions (e.g., leftward taper vs. rightward taper, opposite curvatures, leftward skew vs. rightward skew, and convex vs. concave). Interestingly, using faces that were systematically distorted relative to the average face as adaptors and test stimuli, Leopold et al. recently demonstrated translation tolerant face aftereffects indicative of "contrastive" or opponent coding of face identity in reference to the average face (Leopold, O'Toole, Vetter, & Blanz, 2001; also see Zhao & Chubb, 2001 for scale tolerance and Webster & MacLin, 1999 for the initial demonstration of face aftereffects).

It was suggested (Leopold et al., 2001; Suzuki, 2001; Suzuki & Cavanagh, 1998) that opponent coding of these global shape attributes might occur in the inferotemporal cortex (IT) where cells appear to have tunings for specific shape attributes with varying degrees of position, scale, and surface-feature tolerance (e.g., Fujita, Tanaka, Ito, & Cheng, 1992; Hikosaka, 1999; Ito, Fujita, Tamura, & Tanaka, 1994; Ito, Tamura, Fujita, & Tanaka, 1995; Sáry, Vogels, Kovács, & Orban, 1995; Sato, Kawamura, & Iwai, 1980; see Logothetis & Sheinberg, 1996; Tanaka, 1996, for reviews). Furthermore, similar to the orientation and spatial frequency columns in V1 and V2 (e.g., De Valois, Albrecht, & Thorell, 1982; Foster, Gaska, Nagler, & Pollen, 1985; Hubel & Wiesel, 1968), IT seems to be organized into shape-attribute micro-columns where neighboring columns tend to process similar shape attributes (e.g., Fujita et al., 1992; Tsunoda, Yamane, Nishizaki, & Tanifuji, 2001; Wang, Tanaka, & Tanifuji, 1996; Wang, Fujita, & Maruyama, 2000). As the cells tuned to local orientation and spatial-frequency in V1 and V2 are thought to mediate aftereffects on local image features (figural, spatial-frequency, and direct tilt aftereffects; e.g., Blakemore, Nachmias, & Sutton, 1970; Gibson & Radner, 1937; Kohler & Wallach, 1944; see Braddick, Campbell, & Atkinson, 1978 and Wenderoth & van der Zwan, 1989 for reviews), shape-attribute-tuned cells in IT might mediate opponent aftereffects on global shape attributes.

The fact that opponent shape aftereffects are strongly modulated by attention suggests that activity and adaptation of these hypothesized shape-attribute-tuned neural units are attention sensitive. In contrast, attention seems to have only a minor effect on adaptation at the initial stage of pattern processing (e.g., in V1) as conventional direct tilt aftereffects (reflecting local orientation adaptation) were only weakly modulated by attention (measured using overlapped left-tilted and right-tilted gratings, and using prolonged [60 s] adaptation, Spivey & Spirn, 2000). This study thus investi-

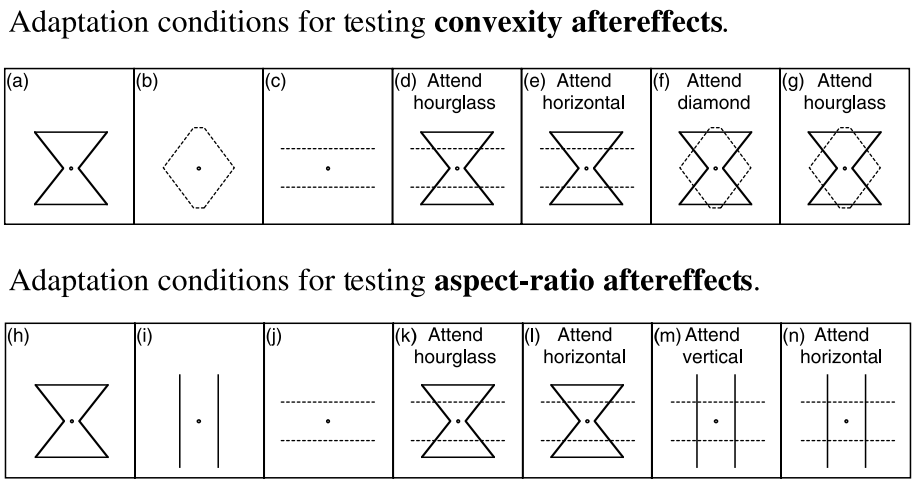

Fig. 2. The seven adaptation conditions used to measure attentional modulations of convexity aftereffects (a)–(g) and aspect-ratio aftereffects (h)–(n). The solid and dotted lines indicate different colors (see text for details).

gated the possibility that strong attentional modulation of opponent shape aftereffects might be primarily due to direct weighting of opponent-shape-coding activity.

To describe the aftereffects examined here, convexity aftereffects were measured as illustrated in Fig. 1a (as in Suzuki, 2001). The (concave) hourglass adaptor induced a convex distortion (Fig. 1a, top), whereas the (convex) diamond adaptor induced a concave distortion (Fig. 1a, bottom) on the test pattern. Aspect-ratio aftereffects were measured using the same test pattern (Fig. 1b). The horizontal adaptor induced vertical elongation (Fig. 1b, top), whereas the vertical adaptor induced horizontal elongation (Fig. 1b, bottom) on the test pattern. Attentional modulation of these aftereffects was measured by using overlapped adaptors. Prior results demonstrated substantial attentional modulation (40–60% relative to perfect selection estimated with singly presented adaptors) for an overlapped hourglass/diamond adaptor (Fig. 2f and g, Suzuki, 2001) and for an overlapped horizontal/vertical adaptor (Fig. 2m and n, pilot results). For example, when observers were instructed to attend [2] to the (concave) hourglass in the overlapped hourglass/diamond adaptor, the test pattern tended to appear convex, whereas when observers attended to the (convex) diamond, the test pattern tended to appear concave.

Linear attention weights were used to quantify attentional modulation to facilitate comparison with neurophysiological results (e.g., Reynolds, Chelazzi, & Desimone, 1999). For example, consider evaluation of attentional modulation of convexity aftereffects for an overlapped hourglass/diamond adaptor (Fig. 2f and g). The baseline aftereffects were first measured with the hourglass adaptor presented alone (referred to as H) and with the diamond adaptor presented alone (referred to as D). If attention linearly weighted contour inputs from the attended and ignored shapes, the resultant aftereffect should be a linear combination of the baseline aftereffects. That is

$$[\text{Attend hourglass aftereffect}] = w_{\text{H/D}} \cdot H + (1 - w_{\text{H/D}}) \cdot D + [\text{other effects}] \quad (1)$$

and

$$[\text{Attend diamond aftereffect}] = w_{\text{D/H}} \cdot H + (1 - w_{\text{D/H}}) \cdot D + [\text{other effects}], \quad (2)$$

where w's are *linear attention weights for the hourglass contours* with the first subscript indicating the attended shape and the second subscript indicating the ignored shape (e.g., H/D for hourglass being attended against diamond). Note that *attention weights for the diamond contours are expressed as* $(1 - w)$'s because attention weights for the two overlapped shapes should add up to 1. The *other effects* represent potential contributions from global processing of the overlapped hourglass/diamond stimulus (i.e., contributions that cannot be explained by linear weighting of aftereffects from individual shapes).

[2] Observers found attending to one of the overlapped shapes relatively easy while failure to do so was noticeable. The strong attentional modulation of shape aftereffects obtained also verified that observers were successful in selectively attending to a particular shape. Numerous prior studies also manipulated attention by instructing observers to attend, including classic studies using central cues (e.g., Posner, Snyder, & Davidson, 1980), studies measuring attention operation characteristic curves to infer resource bottlenecks while observers divided attention between stimuli at various ratios (e.g., Sperling & Melchner, 1978; Lee, Koch, & Braun, 1999), as well as many studies measuring attentional modulation of various aftereffects (e.g., Lankheet & Verstraten, 1995; Mukai & Watanabe, 2001; Spivey & Spirn, 2000; Suzuki & Cavanagh, 1997; Von Grünau, Bertone, & Pakneshan, 1998). An fMRI study further demonstrated that instructions alone produced attentional modulation of neural responses in MT-MST (O'Craven, Rosen, Kwong, Treisman, & Savoy, 1997). Thus, instructing observers to attend is a valid and effective method for manipulating attention.

It is reasonable to assume that these global effects depend on the specific stimulus configuration, and therefore are equivalent whether observers attend to the hourglass or to the diamond. Then, subtracting Eq. (2) from Eq. (1) yields

$$w_{H/D} - w_{D/H} = \frac{[\text{attend hourglass aftereffect}] - [\text{attend diamond aftereffect}]}{H - D} \quad (3)$$

This is an expression for the difference in attention weights (differential attention weights) for the hourglass contours between when they are attended and when they are ignored (i.e., when diamond contours are attended). Because the differential attention weight is identical for the diamond contours (i.e., $[1 - w_{D/H}] - [1 - w_{H/D}] = w_{H/D} - w_{D/H}$), Eq. (3) can be generalized as

$$w_{\text{attended}} - w_{\text{ignored}} = \frac{[\text{attend X aftereffect}] - [\text{attend Y aftereffect}]}{[\text{X alone aftereffect}] - [\text{Y alone aftereffect}]} \quad (4)$$

where X and Y could be any pair of shapes. Further, $w_{\text{attended}} - w_{\text{ignored}}$ also represents the proportion of attentional modulation relative to the maximum possible modulation estimated from fully attending to each shape presented alone.

Two distinct hypotheses were considered for the mechanism of substantial attentional modulation of brief convexity and aspect-ratio aftereffects. First, attention might generally weight the selected contours more heavily than the ignored contours—*the contour-weighting hypothesis*. According to this hypothesis, given that observers exert an equivalent degree of attentional effort (per instruction to attend maximally to the specific shape), the relative weighting of the attended and ignored contours should be independent of the particular shape aftereffects examined (e.g., convexity or aspect-ratio aftereffects) and independent of the particular combinations of adaptor shapes tested; thus, all adaptor pairs shown in Fig. 2d–g and k–n should yield equivalent attentional modulation.

Alternatively, attentional modulation of opponent shape aftereffects might be opponency specific. Note that when strong attentional modulations of convexity and aspect-ratio aftereffects were previously demonstrated, the adaptor always consisted of overlapped opponent shapes that produced opposite aftereffects (i.e., overlapped convex and concave shapes, or overlapped tall and flat shapes). Thus, it is possible that attention might modulate opponent shape aftereffects *primarily by swaying the balance of opponent activity (between the opposite-tuned populations of neural units) within opponent coding of the attended shape attribute—the opponent-level-modulation hypothesis*. For example, attending to a concave component of a pattern might sway the balance of opponent activity within the opponent coding of convexity, enhancing the activity of concave-tuned units and suppressing the activity of convex-tuned units, while leaving units involved in coding other orthogonal shape attributes, such as aspect ratio, unaffected. Such attentional enhancements of "lateral inhibition" at the level of opponent shape coding might be mediated by local inhibitory interactions among shape-attribute micro-columns in IT (e.g., Wang et al., 2000), though direct physiological evidence of opponent coding of shape attributes and of interactions among opponent-tuned units has yet to emerge.

The opponent-level-modulation hypothesis also embodies a broader question of whether an ignored shape attribute can be automatically encoded when it does not compete with the attended feature. When two opponent shapes are paired, attending to one feature value must necessarily suppress the opposite feature value. For example, convexity and concavity (or horizontal and vertical elongation) cannot be encoded simultaneously because they are mutually exclusive. However, when the horizontal adaptor is paired with the hourglass adaptor (e.g., Fig. 2d, e, k, and l), for example, the image contains a horizontally elongated component and a concave component, which are not mutually exclusive. There is no a priori reason to presume that these non-canceling (geometrically orthogonal) attributes cannot be encoded in parallel by an aspect-ratio coding mechanism and by a convexity-coding mechanism, respectively. Attending to the horizontal elongation component of the image, for example, does not necessarily have to reduce simultaneous encoding of the concave component. This possibility of "free encoding" *of an ignored orthogonal attribute* is captured by the opponent-level-modulation hypothesis in its assumption that *attention operates within opponent coding of the attended shape attribute without affecting encoding of orthogonal shape attributes*. As illustrated in Fig. 3, because of this critical assumption, the opponent-level-modulation hypothesis predicts that attentional modulation of shape aftereffects should be strong for an opponent pair, but weak for a non-opponent pair.

In Fig. 3a, the overlapped (concave) hourglass and (convex) diamond form an *opponent adaptor* (shown at top). Attention to the concave hourglass is predicted to sway the balance of responses within the opponent coding of convexity in favor of concave-tuned units (thick arrows), resulting in enhanced responses for the concave-tuned units (upward arrow triplets) and suppressed responses for the convex-tuned units (downward arrow triplets). This concave dominant activity in the opponent coding of convexity during adaptation should tip the post-adaptation sensitivity balance in the opposite direction (indicated as "Concave adapted"). Thus, attending to the (concave) hourglass adaptor should increase the subsequent relative sensitivity of convex-

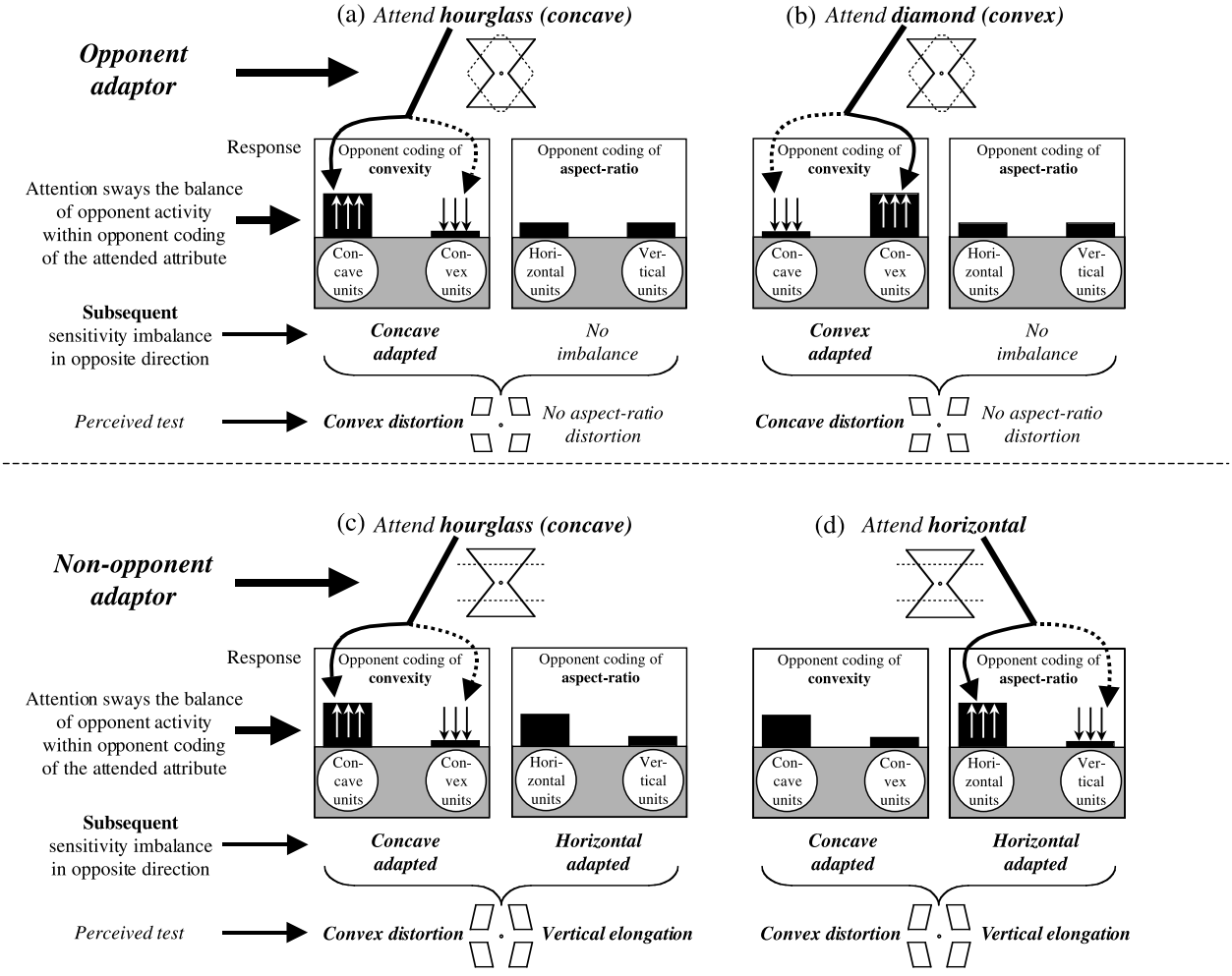

Fig. 3. An illustration of the predictions of *the opponent-level-modulation hypothesis*; *attention sways the balance of opponent activity (between the opposite-tuned populations of neural units) within opponent coding of the attended shape attribute, but without affecting neural activity for coding other shape attributes*. The small left panels show responses of the hypothetical concave-tuned and convex-tuned neural units within the opponent coding of convexity. The small right panels show responses of the hypothetical horizontal-elongation-tuned and vertical-elongation-tuned neural units within the opponent coding of aspect ratio. (a) and (b) predictions for an *opponent adaptor* when the (concave) hourglass is attended (a) and when the (convex) diamond is attended (b). (c) and (d) predictions for a *non-opponent adaptor* when the (concave but aspect-ratio neutral) hourglass is attended (c) and when the (horizontally elongated but convexity neutral) horizontal lines are attended (d). See text for details.

tuned units, making the symmetric test pattern appear convex (indicated as "Convex distortion"). The activity of the aspect-ratio tuned units should remain at the baseline level (equal baseline responses for the horizontal-tuned and vertical-tuned units, indicated as "No imbalance") because the adaptor is adjusted to have a neutral aspect ratio. Thus, no aspect-ratio based distortion (vertical or horizontal elongation) should be induced on the test pattern (indicated as "No aspect-ratio distortion"). Similarly, as shown in Fig. 3b, when the (convex) diamond is attended, attention sways the balance of responses within the opponent coding of convexity in favor of the convex-tuned units, resulting in a subsequent concave distortion of the test pattern (again, with no aspect-ratio based distortions). Though not shown in Fig. 3, when the adaptor consists of the overlapped vertical and horizontal lines (Fig. 2m and n), aspect-ratio aftereffects should be similarly modulated by attention (via swaying of the relative activity of horizontal-tuned and vertical-tuned units within the opponent coding of aspect ratio) with no induction of convexity aftereffects.

In contrast, when the adaptor consists of overlapped *non-opponent shapes*, the opponent-level-modulation hypothesis predicts that attention effects should be small (Fig. 3c and d). The overlapped (concave) hourglass and horizontal lines formed an appropriate *non-opponent adaptor* because (1) the aspect ratio of the hourglass was adjusted to be neutral (causing no distortion of aspect ratio on the test pattern) and (2) the horizontal lines induced no distortion of convexity on the test pattern. Convexity and aspect-ratio aftereffects are also geometrically orthogonal in that the test pattern can be distorted, for example, to be convex and vertically

elongated at the same time (with no cancellation). Because the hourglass/horizontal adaptor contains a concave component (with no opposing convex components) and a horizontally elongated component (with no opposing vertically elongated components), it should activate concave units more than convex units in the opponent coding of convexity and should activate horizontal units more than vertical units in the opponent coding of aspect ratio. Thus, the opponent responses are already tipped towards the concave units and the horizontal units without selective attention. Attention to the (concave) hourglass adaptor, for example, may enhance the dominance of concave units over convex units within the coding of convexity, but without affecting the dominance of horizontal units over vertical units within the coding of aspect ratio (Fig. 3c). Similarly, attention to the horizontal adaptor may enhance the dominance of horizontal units over vertical units within the coding of aspect ratio, but without affecting the dominance of concave units over convex units within the coding of convexity (Fig. 3d). Thus, both a convex aftereffect and a vertical-elongation aftereffect should be induced simultaneously on the test pattern (see ''Perceived test'' at the bottom of Fig. 3), regardless of whether the hourglass adaptor (Fig. 3c) or the horizontal adaptor (Fig. 3d) is attended. Even if the convex distortion is relatively greater when the hourglass adaptor is attended and the vertical elongation is relatively greater when the horizontal adaptor is attended due to attentional enhancement of the pre-existing response imbalance (arrow triplets), attention effects here should be small compared to when attention reverses the balance of activity in opposite directions as in the case of opponent adaptors (Fig. 3a and b).

These predictions of the opponent-level-modulation hypothesis can also be expressed in terms of attention weights; *attending to a particular shape feature should substantially down-weight its opponent feature, but should not down-weight other non-opponent shape features*. For example, within the opponent coding of convexity, attending to the (convex) diamond should substantially down-weight the opponent (concave) activity from the ignored hourglass (Fig. 3b, left panel), whereas attending to the (convexity-neutral) horizontal lines should not down-weight the concave activity from the ignored hourglass (Fig. 3d, left panel); that is, $w_{D/H} < w_{HZ/H}$, where $w_{D/H}$ and $w_{HZ/H}$ indicate attention weights for the ignored hourglass when the diamond and the horizontal lines are attended, respectively. In contrast, the contour-weighting hypothesis predicts that attention weights are shape independent, that is, $w_{D/H} \sim w_{HZ/H}$. In the opponent-level-modulation hypothesis (as well as in the contour-weighting hypothesis), weighting of the attended shape is assumed to be relatively constant irrespective of the ignored shape; that is, $w_{H/D} \sim w_{H/HZ}$, where $w_{H/D}$ and $w_{H/HZ}$ indicate attention weights for the attended hourglass when the diamond and the horizontal lines are ignored, respectively. Thus, for attentional modulation of convexity aftereffects, the opponent-level-modulation hypothesis predicts, $w_{H/D} - w_{D/H} > w_{H/HZ} - w_{HZ/H}$ (i.e., greater attentional modulation for the opponent adaptor (Fig. 2f and g) than for the non-opponent adaptor (Fig. 2d & e)), whereas the contour-weighting hypothesis predicts, $w_{H/D} - w_{D/H} \sim w_{H/HZ} - w_{HZ/H}$ (i.e., equivalent attentional modulation for the two types of adaptor). Similar predictions can be derived for attentional modulation of aspect-ratio aftereffects.

To summarize, the contour-weighting hypothesis predicts that brief shape aftereffects should be attentionally modulated regardless of the measured aftereffect and of the opponency of adaptors. In contrast, the opponent-level-modulation hypothesis predicts that shape aftereffects should be attentionally modulated primarily with opponent adaptors.

2. Experiment

Convexity aftereffects were measured under seven conditions (Fig. 2a–g), (1) the hourglass adaptor presented alone, (2) the diamond adaptor presented alone, (3) the horizontal adaptor presented alone, (4) attention to the hourglass in the overlapped hourglass/horizontal adaptor, (5) attention to the horizontal lines in the overlapped hourglass/horizontal adaptor, (6) attention to the diamond in the overlapped hourglass/diamond adaptor, and (7) attention to the hourglass in the overlapped hourglass/diamond adaptor. Similarly, aspect-ratio aftereffects were measured under the equivalent conditions (Fig. 2h–n), (1) the hourglass adaptor presented alone, (2) the vertical adaptor presented alone, (3) the horizontal adaptor presented alone, (4) attention to the hourglass in the overlapped hourglass/horizontal adaptor, (5) attention to the horizontal lines in the overlapped hourglass/horizontal adaptor, (6) attention to the vertical lines in the overlapped horizontal/vertical adaptor, and (7) attention to the horizontal lines in the overlapped horizontal/vertical adaptor.

On the basis of the resulting data, the degree of attentional selection (measured as $w_{attended} - w_{ignored}$; see Eq. (4)) was computed for the opponent adaptors (Fig. 2f–g and m–n) and for the non-opponent adaptors (Fig. 2d–e and k–l) for convexity and aspect-ratio aftereffects. The degree of opponency of the overlapped shapes was also quantified with respect to convexity and aspect ratio. For convexity aftereffects, *% convexity-opponency* for the hourglass/diamond adaptor (opponent adaptor) was computed as, [diamond-alone *convexity aftereffect*]/[hourglass -*alone convexity aftereffect*] × 100%. The convexity-opponency in this case was expected to be near 100% because the diamond adaptor tended to produce

convexity aftereffects that were similar in magnitude but opposite in direction to those produced by the hourglass adaptor. Similarly, % convexity-opponency for the hourglass/horizontal adaptor (non-opponent adaptor) was computed as, [horizontal-alone convexity aftereffect]/[hourglass -*alone convexity aftereffect*] × 100%. The convexity-opponency in this case was expected to be near 0% because the horizontal adaptor tended to produce *no* convexity aftereffects. For aspect-ratio aftereffects, *% aspect-ratio-opponency* for the horizontal/vertical adaptor (opponent adaptor) was computed as, [vertical-alone aspect-ratio aftereffect]/[horizontal-alone aspect-ratio aftereffect] × 100%. The aspect-ratio-opponency in this case was expected to be near 100% because the vertical adaptor tended to produce aspect-ratio aftereffects that were similar in magnitude but opposite in direction to those produced by the horizontal adaptor. Percent aspect-ratio-opponency for the hourglass/horizontal adaptor (non-opponent adaptor) was computed as, [hourglass-alone aspect-ratio aftereffect]/[horizontal-alone aspect-ratio aftereffect] × 100%. The aspect-ratio-opponency in this case was expected to be near 0% because the hourglass adaptor was adjusted to produce *no* (or minimal) aspect-ratio aftereffects (i.e. the hourglass adaptor was adjusted to produce only a convexity aftereffect). The % opponency was given a positive sign when the overlapped shapes produced aftereffects in opposite directions, whereas it was given a negative sign when the overlapped shapes produced aftereffects in the same direction. The latter occurred for non-opponent pairs in some cases. For example, though the horizontal adaptor produced little convexity aftereffects overall, it produced small concave or convex distortion in each measurement.

It was then determined whether the degree of attentional selection ($w_{\text{attended}} - w_{\text{ignored}}$) depended on the degree of opponency for convexity aftereffects and aspect-ratio aftereffects. To reiterate the predictions, the contour-weighting hypothesis predicted that the degree of attentional modulation should be largely invariant regardless of the type of aftereffects measured and of the opponency of the overlapped adaptors. In contrast, the opponent-level-modulation hypothesis predicted that the degree of attentional modulation should be much greater when opponency was near 100% than when opponency was near 0%.

2.1. Method

Observers. Three experienced psychophysical observers participated (the author and 2 naïve observers). All had normal or corrected-to-normal vision, and were tested under normal lighting conditions.

Apparatus. Stimuli were shown on a 17-in. color monitor (75 Hz) and the experiments were controlled by an Apple PowerMac 8600/300 MHz with Vision Shell software (*Micro ML*).

Stimuli. The test pattern consisted of a square array of four squares (Fig. 1); the sides of the squares as well as the edge-to-edge distance between the squares were 3.4°. While the skew and aspect-ratio of the squares were varied to cancel convexity and aspect-ratio aftereffects using a staircase procedure (described below), the area and center positions of the squares were kept constant.

The hourglass adaptor was 13.5° tall; the diamond adaptor was about 10% taller so that its top and bottom contours did not exactly overlap the hourglass contours when the two shapes were superimposed. The angle of the side contours (relative to vertical) was fine-tuned for each observer so that the hourglass adaptor did not produce aspect-ratio aftereffects, but so that the side contours always went through the locations of the centers of the test squares. The overall scale of the hourglass and diamond adaptors and the test pattern were made similar because convexity aftereffects were largest when the adaptor was about the same size as (or slightly larger than) the test pattern (Suzuki, 2001). It was important to maximize baseline aftereffects so that attentional modulation could be measured with high sensitivity. Although contours of the adaptor and the test pattern were not widely separated, the hourglass/diamond aftereffects reported here were likely to be global aftereffects of convexity rather than the sum of local tilt aftereffects. This is because, in prior studies (Rivest et al., 1998; Suzuki, 2001), (1) convexity aftereffects as well as aspect-ratio and taper aftereffects diminished rather gradually when the adaptor was reduced in size (with the test pattern held constant), and convexity aftereffects (illustrated in Fig. 1a) in particular persisted even when the small adaptor fit completely inside the central space enclosed by the four test squares, and (2) oriented line textures covering the region of the test pattern (suited for inducing local tilt aftereffects) produced virtually no aftereffects with the brief stimulus sequence used.

The horizontal and vertical adaptors used for measuring aspect-ratio aftereffects were modified relative to those used in the previous studies (e.g., a single rectangular bar, an ellipse with various aspect ratios, or a line with various lengths). Though aspect-ratio aftereffects were demonstrated even when the adaptor was displaced by as much as 12° or scaled by 0.3–1.8 relative to the test pattern, the aftereffects tended to be largest when the adaptor and the test pattern were both centered at the same location, and when the adaptor was more elongated (e.g., Rivest et al., 1997; Suzuki & Cavanagh, 1998; Suzuki & Rivest, 1998). Thus, to maximize baseline aspect-ratio aftereffects, the adaptors used were a pair of long (14.7°) parallel lines (vertical or horizontal) which went through the locations of the centers of the test squares (Fig. 1b). Suzuki and Cavanagh (1998) have

demonstrated that even when a line adaptor overlaps a test pattern, the aftereffects induced with brief stimulus sequences are likely to be aspect-ratio-based aftereffects which cannot be explained on the basis of asymmetric size aftereffects occurring along vertical and horizontal orientations.

All shapes were drawn with 0.06° thick lines. The adaptors were drawn with bright contours (21.5 cd/m^2) against a black background (4.1 cd/m^2; all color guns turned off), whereas the test pattern was drawn with black contours (4.1 cd/m^2) against a white background (89.0 cd/m^2; all color guns turned on, CIE[0.283,0.299]). The contrast was thus 0.68 for the adaptors and −0.91 for the test pattern (computed as $[L_{\text{line}} - L_{\text{background}}]/[L_{\text{line}} + L_{\text{background}}]$). The contrast polarity was reversed between adaptation and test to reduce any sensation of apparent motion between the adaptor and the test pattern as in Suzuki (1999, 2001). When the adaptor consisted of overlapped shapes (Fig. 2d–g and k–n), the two shapes were colored differently, one red (CIE[0.592,358]) and the other green (CIE[0.332,0.546]), to facilitate perceptual segregation of the overlapped shapes, and thus to facilitate attentional selection (e.g., Suzuki & Grabowecky, 2000; Suzuki, 2001). When there was only one adaptor shape, its color was either red or green. The viewing distance was 76 cm.

Procedure. A trial began with a warning beep and a presentation of a blank white screen with a small gray fixation circle (diameter = 0.12°) at the center (Fig. 4). After 1342 ms, an adaptor was presented for 134 ms (against a black background), followed by a 201 ms blank white screen, then by the brief test pattern (27 ms) which was immediately followed by a full-screen random-dot mask (403 ms; bright dots = 89.0 cd/m^2 and dark dots = 4.1 cd/m^2; dot size = 0.06° × 0.06°). In trials measuring convexity aftereffects, observers responded as to whether the test pattern appeared overall convex or concave in a forced choice manner (they were instructed to ignore any apparent horizontal or vertical elongation of the squares). In trials measuring aspect-ratio aftereffects, observers responded as to whether the "squares" of the test pattern appeared horizontally or vertically elongated in a forced choice manner (they were instructed to ignore any apparent convexity or concavity of the test pattern).

A staircase method was used to estimate the magnitude of the convexity aftereffect or the aspect-ratio aftereffect. Two interleaved staircases alternated across trials. When convexity aftereffects were measured, one staircase started at $\theta = +1.91°$ (the test pattern appearing clearly convex without adaptation), whereas the other staircase started at $\theta = -1.91°$ (the test pattern appearing clearly concave without adaptation); the θ was measured relative to vertical (see Fig. 4). Each "convex" response made the test pattern in the following trial for the corresponding staircase less convex by approximately 0.48°; similarly, each "concave" response made the subsequent test pattern more convex by 0.48°. The values of the last six reversals for the two staircases (12 reversals total) were averaged to estimate the magnitude of the convexity aftereffect (i.e., the degree of θ required to cancel the aftereffect). Aspect-ratio aftereffects were measured similarly. One staircase started at log aspect ratio (LAR) (defined as, natural-log{[vertical length]/[horizontal length]}) = +0.0667 (the test "squares" appearing clearly vertically elongated without

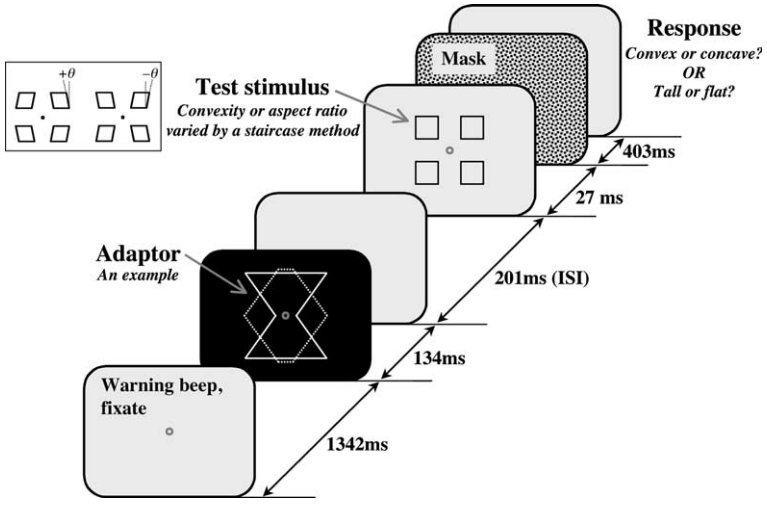

Fig. 4. Sequence of events in an experimental trial. At the end of each trial, observers responded whether the test pattern appeared convex or concave (when convexity aftereffects were measured) or whether the "squares" of the test pattern appeared horizontally or vertically elongated (when aspect-ratio aftereffects were measured) in a forced choice manner. A staircase procedure adjusted the orientation (θ) of the vertical lines of the test squares (when convexity aftereffects were measured) or adjusted the aspect ratio of the test squares (when aspect-ratio aftereffects were measured) appropriately to cancel out the convexity/concavity or the horizontal/vertical-elongation induced by the aftereffects. The solid and dotted contours of the adaptor figure indicate different colors.

adaptation), whereas the other staircase started at LAR = −0.0667 (the test "squares" appearing clearly horizontally elongated without adaptation). Each "vertically elongated" response reduced LAR for the test pattern in the following trial for the corresponding staircase by approximately 0.0168; similarly, each "horizontally elongated" response increased LAR for the subsequent test pattern by 0.0168. Again, the values of the last six reversals for the two staircases (12 reversals total) were averaged to estimate the magnitude of the aspect-ratio aftereffect (i.e., the degree of aspect ratio, LAR, required to cancel the aftereffect). [3]

A pilot experiment was first conducted to adjust the angle of the hourglass adaptor such that it produced minimal aspect-ratio aftereffects on average. For one observer, the side contours were tilted 35° from vertical and for the remaining observers, they were tilted 40° from vertical. The contours of the diamond adaptor were tilted by the same angle but in the opposite direction. As expected, the horizontal adaptor did not produce any convexity aftereffects. As indicated in the results section (Fig. 5a), the adaptors did generate the desired degrees of opponency, near 0% and near 100%, on average.

Convexity and aspect-ratio aftereffects were measured in the corresponding sets of seven conditions (Fig. 2a–g for convexity aftereffects and Fig. 2h–n for aspect-ratio aftereffects). In each session, one type of aftereffect (either convexity or aspect-ratio) was tested in all seven conditions, with at least a 5-min break between conditions. Each type of aftereffect was tested in four sessions to counterbalance for color assignments (red/green for the hourglass and green/red for the diamond and the horizontal adaptors for measuring convexity aftereffects [Fig. 2a–g], and red/green for the horizontal and green/red for the vertical and the hourglass adaptors for measuring aspect-ratio aftereffects [Fig. 2h–n]) and for the testing order (as shown in Fig. 2 or in the reversed order within the single-shape and within the overlapped-shape conditions; the single-shape conditions were always tested first). There were thus a total of eight sessions (the two types of aftereffect measured and the four counterbalancing repetitions described above). Aspect-ratio aftereffects were tested in sessions 1, 2, 5, and 6, and convexity aftereffects were tested in sessions 3, 4, 7, and 8. At least a 1-day break was inserted between sessions. The color assignment was alternated across sessions, and the testing order was reversed in the last four sessions. Note that data from each session yielded two estimates of attentional modulation, $w_{\text{attended}} - w_{\text{ignored}}$ (based on Eq. (4)), one for the opponent adaptor and the other for the non-opponent adaptor (for one type of aftereffect).

2.2. Results

The effectiveness of selective attention (measured as % attentional modulation or $[w_{\text{attended}} - w_{\text{ignored}}] \times 100\%$, Eq. (4)) is plotted for convexity aftereffects (open squares) and aspect-ratio aftereffects (solid squares) as a function of the degree of opponency between the overlapped adaptor shapes (measured as % opponency). In Fig. 5a, the data are averaged across the three observers. The pattern is clear. Attentional modulations were strong (∼60%) independently of the type of shape aftereffect measured and independently of opponency of the overlapped adaptor shapes; attentional modulations were robust and equivalent when the two overlapped shapes produced almost exactly opposite aftereffects (∼100% opponency) and when the two overlapped shapes produced orthogonal aftereffects (∼0% opponency). [4]

A more detailed picture is shown in Fig. 5b. Here, the data from individual experimental sessions are plotted for each observer (open symbols for convexity aftereffects and solid symbols for aspect-ratio aftereffects). Different symbols (circles, squares, and triangles) indicate data from different observers. The plot confirms the average data, shown in Fig. 5a, that the degree of attentional modulation remained relatively constant as the opponency of the overlapped shapes widely varied (due to the opponency manipulation and to random variability in the magnitude of baseline aftereffects). The slopes of the regression lines (dotted line for convexity aftereffects and solid line for aspect-ratio aftereffects) were not significantly different from zero (based on $p < 0.05$ criterion); this was the case even when the regression lines were examined separately for the individual observers.

[3] Because the magnitudes of aspect-ratio aftereffects were modest (maximum induced aspect ratio of 1.31), the results regarding their attentional modulations were virtually identical whether aspect-ratio aftereffects were measured in LAR (natural log aspect ratio) or in raw aspect ratio (expressed as proportion of elongation = {[longer axis]/[shorter axis]} − 1, with a positive sign given to vertical elongation and a negative sign given to horizontal elongation). Greater aspect ratios are slightly more exaggerated in raw aspect ratio than in LAR; thus, the baseline aftereffects (with singly presented adaptors) were slightly larger when measured in raw aspect ratio than when measured in LAR. Because of this, the obtained attentional modulations (Fig. 5) would be smaller by about 1% on average if raw aspect ratio was used instead of LAR.

[4] The average baseline aftereffects were, 1.45° (SE = 0.17°) for the convex distortion induced by the (concave) hourglass adaptor alone, −1.59° (SE = 0.26°) for the concave distortion induced by the (convex) diamond adaptor alone, LAR (natural-log aspect ratio) of 0.19 (SE = 0.04) for the vertical elongation induced by the horizontal adaptor alone (corresponding to 21% elongation of vertical axis relative to horizontal axis), and LAR of −0.14 (SE = 0.02) for the horizontal elongation induced by the vertical adaptor alone (corresponding to 15% elongation of horizontal axis relative to vertical axis).

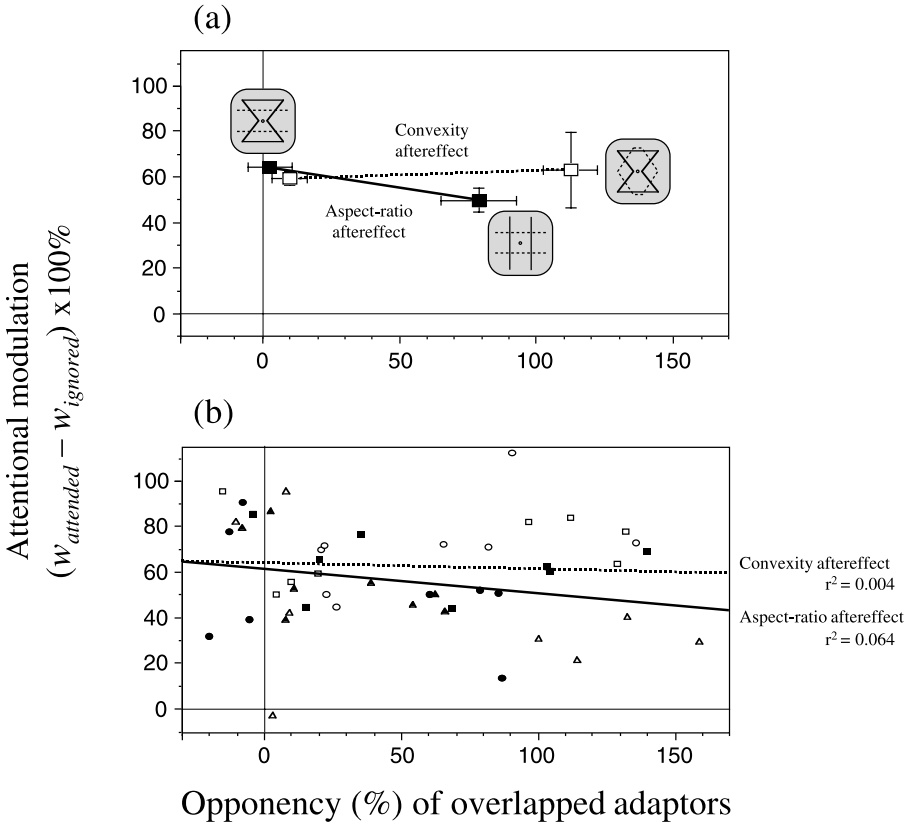

Fig. 5. The effectiveness of selective attention (measured as % attentional modulation = $[w_{\text{attended}} - w_{\text{ignored}}] \times 100\%$, Eq. (4)) is plotted for convexity aftereffects (open symbols and dotted lines) and for aspect-ratio aftereffects (filled symbols and solid lines) as a function of the degree of opponency between the overlapped adaptor shapes (measured as % opponency). (a) Average data. The error bars represent ±1 SE using observers as the random effect. The solid and dotted contours of the adaptor figures indicate different colors. (b) The same data plotted for individual experimental sessions for each observer; different symbols (circles, squares, and triangles) indicate different observers.

The result thus supports the contour-weighting hypothesis; contours were weighted approximately 60% more when they were attended than when they were ignored, independently of the type of aftereffects measured and independently of the figural opponency between the overlapped adaptor shapes.

3. Discussion

Attentional modulation of convexity and aspect-ratio aftereffects was examined using overlapped adaptors and rapid stimulus sequences. Strong attentional modulation previously demonstrated for convexity aftereffects (Suzuki, 2001) was extended to aspect-ratio aftereffects. More important, opponent adaptors (overlapped shapes generating opposite aftereffects) and non-opponent adaptors (overlapped shapes generating orthogonal aftereffects) were used to contrast two potential mechanisms mediating this substantial attentional modulation of brief shape aftereffects. According to the contour-weighting hypothesis, attentional modulation primarily occurs at the stage of general contour processing such that inputs from the attended contours are weighted more heavily than inputs from the ignored contours. According to the opponent-level-modulation hypothesis, attentional modulation primarily occurs within opponent coding of the attended attribute such that responses of units tuned to the attended shape polarity (e.g., convexity) are enhanced and responses of units tuned to the opposite shape polarity (e.g., concavity) are suppressed, while responses of units involved in coding of other orthogonal shape attributes (e.g., aspect ratio) are unaffected.

The results supported the contour-weighting hypothesis by demonstrating that attentional modulation was relatively constant whether convexity aftereffects or aspect-ratio aftereffects were measured, and whether the overlapped adaptor shapes were opponent (opponency ~100%) or non-opponent (opponency ~0%). The contours belonging to each shape were weighted about 60% more when that shape was attended than when the other overlapped shape was attended. The primary prediction of the opponent-level-modulation hypothesis, that attending to a shape feature should substantially down-weight its opponent feature without down-weighting other non-opponent shape features, was rejected. On the contrary, attending to a particular shape feature (e.g.,

concave hourglass) equally down-weighted both its opponent feature (e.g., convex diamond) and a non-opponent feature (e.g., horizontally elongated lines). In a broader conceptual sense, to the degree that brief shape adaptation is a direct consequence of shape encoding, the results suggest that when an observer attends to a particular geometric feature (such as concavity), another simultaneously present geometric feature (such as horizontal elongation) is not encoded "for free" even when the latter does not compete with the attended feature and thus could theoretically be encoded in parallel.

Note that though the current results are consistent with the contour weighting hypothesis and inconsistent with the opponent-level-modulation hypothesis, they do not necessarily favor any particular operational locus of attention. For example, the results are indifferent as to whether attentional modulation occurred at low-level contour processing or at high-level global shape processing so long as attentional selection was due to a general, shape independent, form of linear differential weighting of attended and ignored image parts. Nevertheless, as discussed below, a comparison with neurophysiological results might suggest that the degree of attentional selection obtained in this study could be accounted for on the basis of the degree of attentional selection of oriented contours accomplished at the level of V4 or earlier.

The contour-weighting model of selective attention considered in evaluating the current behavioral data (Eqs. (1)–(4)) is a variant of *the biased competition model* previously proposed to model attentional modulation of neural responses when two competing stimuli were presented within a cell's receptive field in V2 or V4 (e.g., Desimone & Duncan, 1995; Reynolds et al., 1999; also see Luck, Chelazzi, Hillyard, & Desimone, 1997; Moran & Desimone, 1985 for earlier proposals). In particular, both in the current experiment and in Reynolds et al. (1999), $w_{\text{attended}} - w_{\text{ignored}}$, was computed in a similar way, with Reynolds et al. using attentional modulation of neural responses as the dependent measure, whereas it was computed here using attentional modulation of shape aftereffects as the dependent measure. Reynolds et al. obtained population values of, $w_{\text{attended}} - w_{\text{ignored}}$, to be 45% in V2 and 62% in V4 for those cells that showed significant attentional modulation (the values reduced to 33% in V2 and 40% in V4 when all recorded cells were included). Furthermore, $w_{\text{attended}} - w_{\text{ignored}}$, was largely similar across the recorded cells for different stimulus combinations (as indicated by the linear relationships between "Sensory interaction" and "Selectivity" shown in Figs. 10 and 11 in Reynolds et al., 1999). Thus, the relatively constant attentional modulation ($w_{\text{attended}} - w_{\text{ignored}} \sim 60\%$) of shape aftereffects obtained here for different shape combinations could potentially be mediated by attentional modulation of processing at the level of V4.

Besides the obvious fact that Reynolds et al. measured attentional modulation of neural responses whereas attentional modulation of behavioral shape aftereffects was measured here, there were some additional differences between the two studies. First, pairs of stimuli used by Reynolds et al. (variously oriented bars) were non-overlapped. However, though the overall shapes were overlapped in the current study, their contours were non-overlapped except at the intersections (see Fig. 2). The size ($\sqrt{\text{area}}$) of V4 receptive fields increases approximately linearly from about 1° at 1° eccentricity to about 5° at 7° eccentricity (e.g., Desimone & Schein, 1987; Gattass, Sousa, & Gross, 1988). Note that the relatively sparse contours of the adaptor shapes used here extended to about 6° eccentricity. Thus, portions of both the attended and ignored contours should have fallen within individual V4 cells' receptive fields, and those contours should have been largely non-overlapped within each receptive field, similar to the stimuli used by Reynolds et al. A second difference was that in Reynold et al.'s study the baseline responses to singly presented stimuli (one stimulus per receptive field) were measured when those stimuli were ignored (i.e., the animal attended to a stimulus outside of the receptive field) whereas in this study the baseline aftereffects to singly presented adaptors were measured under observers' full attention. However, responses of a V4 cell are relatively weakly modulated by attention when only one stimulus is presented within its receptive field (e.g., Luck et al., 1997; Spitzer, Desimone, & Moran, 1988; McAdams & Maunsell, 1999). Therefore, had the baseline responses been measured when the animal fully attended to the baseline stimuli, estimates of attentional modulation in V4 might have been somewhat smaller (due to potentially larger baseline differences or "Selectivity", i.e., a larger denominator in Eq. (4)), but not substantially different from the reported values.

In conclusion, strong attentional modulations of brief shape aftereffects were independent of the two types of aftereffect measured (convexity and aspect-ratio aftereffects) and independent of the opponency of the overlapped adaptors (opponent vs. non-opponent). These results, in combination with the global nature of brief shape aftereffects (e.g., Rivest et al., 1997, 1998; Suzuki & Cavanagh, 1998; Suzuki, 2001), suggest that brief adaptation of shape-attribute coding (perhaps in IT) is strongly modulated by selective attention primarily via differential weighting by a relatively constant factor of the attended and ignored image parts ($w_{\text{attended}} - w_{\text{ignored}} \sim 60\%$). This attentional weighting might primarily occur in earlier visual areas such as V4 as suggested by a comparison with a neurophysiological result by Reynolds et al. (1999). The current results further suggest that attention to one global geometric feature (e.g., concavity) inhibits encoding of another coincident feature (e.g., horizontal elongation) even if

the two geometric attributes are orthogonal and thus could be encoded in parallel.

Acknowledgements

This research was supported by a grant from the National Science Foundation (SBR-9817643). The author is grateful to Charles Chubb, Marcia Grabowecky, Adam Reeves, and David Regan for their helpful comments on earlier versions of the manuscript.

References

Blakemore, C. B., Nachmias, J., & Sutton, P. (1970). The perceived spatial frequency shift: Evidence for frequency selective neurons in the human brain. *Journal of Physiology (London), 210*, 727–750.

Braddick, O., Campbell, F. W., & Atkinson, J. (1978). Channels in vision: Basic aspects. In: R. Held, H. W. Leibowitz, & L. -H. Teuber (Eds.), *Handbook of sensory physiology: Vol. 8. Perception* (pp. 3–38), Berlin: Springer-Verlag.

De Valois, R. L., Albrecht, D. G., & Thorell, L. G. (1982). Spatial frequency selectivity of cells in macaque visual cortex. *Vision Research, 22*, 545–559.

Desimone, R., & Duncan, J. (1995). Neural mechanisms of selective visual attention. *Annual Review of Neuroscience, 18*, 193–222.

Desimone, R., & Schein, S. J. (1987). Visual properties of neurons in area V4 of the macaque: Sensitivity to stimulus form. *Journal of Neurophysiology, 57*(3), 835–868.

Foster, K. H., Gaska, J. P., Nagler, M., & Pollen, D. A. (1985). Spatial and temporal frequency selectivity of neurons in visual cortical areas V1 and V2 of the macaque monkey. *Journal of Physiology, London, 365*, 331–368.

Frome, F. S., Levinson, J. Z., Danielson, J. T., & Clavadetscher, J. E. (1979). Shifts in perception of size after adaptation to gratings. *Science, 206*, 1327–1329.

Fujita, I., Tanaka, K., Ito, M., & Cheng, K. (1992). Columns for visual features of objects in monkey inferotemporal cortex. *Nature, 360*, 343–346.

Gattass, R., Sousa, A. P. B., & Gross, C. G. (1988). Visuotopic organization and extent of V3 and V4 of the macaque. *Journal of Neuroscience, 8*(6), 1831–1845.

Gibson, J. J., & Radner, M. (1937). Adaptation, after-effect and contrast in the perception of tilted lines I. Quantitative studies. *Journal of Experimental Psychology, 20*, 453–467.

Hartmann, L. (1955). Further studies of gamma movement. In W. D. Ellis (Ed.), *A source book of gestalt psychology*. New York: Humanities Press (Original work published 1923).

Hikosaka, K. (1999). Tolerances of responses to visual patterns in neurons of the posterior inferotemporal cortex in the macaque against changing stimulus size and orientation, and deleting patterns. *Behavioral Brain Research, 100*, 67–76.

Hubel, D. H., & Wiesel, T. N. (1968). Receptive fields and functional architecture of monkey striate cortex. *Journal of Physiology, 195*, 215–243.

Ito, M., Fujita, I., Tamura, H., & Tanaka, K. (1994). Processing of contrast polarity of visual images in inferotemporal cortex of the macaque monkey. *Cerebral Cortex, 5*, 499–508.

Ito, M., Tamura, H., Fujita, I., & Tanaka, K. (1995). Size and position invariance of neuronal responses in monkey inferotemporal cortex. *Journal of Neurophysiology, 73*(1), 218–226.

Kohler, W., & Wallach, H. H. (1944). Figural aftereffects: An investigation of visual processes. *Proceedings of the American Philosophical Society, 88*, 269–357.

Lankheet, M. J. M., & Verstraten, F. A. J. (1995). Attentional modulation of adaptation to two-component transparent motion. *Vision Research, 35*(10), 1401–1412.

Lee, D. K., Koch, C., & Braun, J. (1999). Attentional capacity is undifferentiated: Concurrent discrimination of form, color, and motion. *Perception and Psychophysics, 61*(7), 1241–1255.

Leopold, D. A., O'Toole, A. J., Vetter, T., & Blanz, V. (2001). Prototype-referenced shape encoding revealed by high-level aftereffects. *Nature Neuroscience, 4*(1), 89–94.

Logothetis, N. K., & Sheinberg, D. L. (1996). Visual object recognition. *Annual Review of Neuroscience, 19*, 577–621.

Luck, S. J., Chelazzi, L., Hillyard, S., & Desimone, R. (1997). Neural mechanisms of spatial selective attention in areas V1, V2, and V4 of macaque visual cortex. *Journal of Neurophysiology, 77*, 24–42.

McAdams, C. J., & Maunsell, J. H. R. (1999). Effects of attention on orientation-tuning functions of single neurons in macaque cortical area V4. *Journal of Neuroscience, 19*(1), 431–441.

Moran, J., & Desimone, R. (1985). Selective attention gates visual processing in the extrastriate cortex. *Science, 229*, 782–784.

Mukai, I., & Watanabe, T. (2001). Differential effect of attention to translation and expansion on motion aftereffects (MAE). *Vision Research, 41*(9), 1107–1117.

O'Craven, K. M., Rosen, B. R., Kwong, K. K., Treisman, A., & Savoy, R. L. (1997). Voluntary attention modulates fMRI activity in human MT-MST. *Neuron, 18*, 591–598.

Posner, M. I., Snyder, C. R. R., & Davidson, B. J. (1980). Attention and the detection of signals. *Journal of Experimental Psychology: General, 109*, 160–174.

Regan, D., & Hamstra, S. J. (1992). Shape discrimination and the judgment of perfect symmetry: Dissociation of shape from size. *Vision Research, 32*, 1845–1864.

Reynolds, J. H., Chelazzi, L., & Desimone, R. (1999). Competitive mechanisms subserve attention in macaque areas V2 and V4. *Journal of Neuroscience, 19*(5), 1736–1753.

Rivest, J., Intriligator, J. M., Suzuki, S., & Warner, J. (1998). A shape distortion effect that is size invariant. *Investigative Ophthalmology and Visual Science, 39*(Suppl. 4), S853.

Rivest, J., Intriligator, J. M., Warner, J., & Suzuki, S. (1997). Color and luminance combine at a common neural site for shape distortions. *Investigative Ophthalmology and Visual Science, 38*(Suppl. 4), S1000.

Sáry, G., Vogels, R., Kovács, G., & Orban, G. A. (1995). Responses of monkey inferior temporal neurons to luminance-, motion-, and texture-defined gratings. *Journal of Neurophysiology, 73*(4), 1341–1354.

Sato, T., Kawamura, T., & Iwai, E. (1980). Responsiveness of inferotemporal single units to visual pattern stimuli in monkeys performing discrimination. *Experimental Brain Research, 38*, 313–319.

Sperling, G., & Melchner, M. J. (1978). The attention operation characteristic: Some examples from visual search. *Science, 202*, 315–318.

Spitzer, H., Desimone, R., & Moran, J. (1988). Increased attention enhances both behavioral and neuronal performance. *Science, 240*, 338–340.

Spivey, M. J., & Spirn, M. J. (2000). Selective visual attention modulates the direct tilt aftereffect. *Perception and Psychophysics, 62*(8), 1525–1533.

Suzuki, S. (1999). Influences of contexts on a non-retinotopic skew-contrast effect. *Investigative Ophthalmology and Visual Science, 40*(Suppl. 4), S812.

Suzuki, S. (2001). Attention-dependent brief adaptation to contour orientation: A high-level aftereffect for convexity? *Vision Research, 41*(28), 3883–3902.

Suzuki, S., & Cavanagh, P. (1997). Focused attention distorts visual space: An attentioinal repulsion effect. *Journal of Experimental Psychology: Human Perception and Performance, 23*, 443–463.

Suzuki, S., & Cavanagh, P. (1998). A shape-contrast effect for briefly presented stimuli. *Journal of Experimental Psychology: Human Perception and Performance, 24*(5), 1315–1341.

Suzuki, S., & Grabowecky, M. (2000). Attention during adaptation weakens negative afterimages. In *The 41st annual meeting of the Psychonomic Society, New Orleans, LA*.

Suzuki, S., & Rivest, J. (1998). Interactions among aspect-ratio channels. *Investigative Ophthalmology and Visual Science, 39*(Suppl. 4), S855.

Tanaka, K. (1996). Inferotemporal cortex and object vision. *Annual Review of Neuroscience, 19*, 109–139.

Tsunoda, K., Yamane, Y., Nishizaki, M., & Tanifuji, M. (2001). Complex objects are represented in macaque inferotemporal cortex by the combination of feature columns. *Nature Neuroscience, 4*(8), 832–838.

Von Grünau, M. W., Bertone, A., & Pakneshan, P. (1998). Attentional selection of motion states. *Spatial Vision, 11*, 329–347.

Wang, G., Tanaka, K., & Tanifuji, M. (1996). Optical imaging of functional organization in the monkey inferotemporal cortex. *Science, 272*, 1665–1668.

Wang, Y., Fujita, I., & Maruyama, Y. (2000). Neuronal mechanisms of selectivity for object features revealed by blocking inhibition in inferotemporal cortex. *Nature Neuroscience, 3*(8), 807–813.

Webster, M., & MacLin, O. H. (1999). Figural after-effects in the perception of faces. *Psychonomic Bulletin and Review, 6*(4), 647–653.

Wenderoth, P., & van der Zwan, R. (1989). The effects of exposure duration and surrounding frames on direct and indirect tilt aftereffects and illusions. *Perception and Psychophysics, 46*(4), 338–344.

Zhao, L., & Chubb, C. (2001). The size-tuning of the face-distortion after-effect. *Vision Research, 41*, 2979–2994.